Diffusion-Corrected Simultaneous Multilayer Growth Model

Qiang Fu and Thomas Wagner*

Max-Planck-Institut für Metallforschung, Heisenbergstrasse 3, D-70569 Stuttgart, Germany

(Received 28 October 2002; published 14 March 2003)

A diffusion-corrected simultaneous multilayer (DCSM) model was developed, taking into account up-step and down-step diffusion of adatoms and enabling rapid identification of different film growth modes. This DCSM model was applied to the initial growth of Cr on (100) $SrTiO_3$ and (0001) α-Al_2O_3 surfaces, monitoring the deposition process by *in situ* Auger electron spectroscopy. We conclude with general remarks on the usefulness of the DCSM model for exploiting solid state wetting processes of thin metal films on different substrates.

DOI: 10.1103/PhysRevLett.90.106105 PACS numbers: 68.55.Jk, 68.43.Jk, 79.20.–m

Various surface science techniques can be applied to study the growth modes of thin films. For example, low-energy ion scattering (LEIS) and scanning probe microscopy techniques have been used in a variety of studies allowing a direct determination of the growth mode [1–6]. Because of its simplicity, Auger electron spectroscopy (AES) is still widely recognized as an effective and popular tool for the determination of growth modes. Until now, most of the investigations concerning the determination of film growth modes are conducted by AES (e.g., [7,8]). To extract the growth mode from the AES curves, one generally follows a procedure described by Rhead *et al.* [9], which allows one to distinguish between the Frank–van der Merwe (FM), Stranski-Krastanov (SK), Volmer-Weber (VW), and simultaneous multilayer (SM) growth modes. In case of FM growth characteristic breaks are present in the intensity-thickness curves, whereas in case of SK growth a single break is expected. In contrast, the curves for VW or SM growth are nonlinear or exponential (compare Figs. 1 and 2 in [9]). The scattering of the experimental data, a limited number of data points, and a weak attenuation of the AES signals makes it sometimes hard to detect the characteristic breaks for the FM growth mode. Furthermore, for a variety of systems, e.g., metal/oxide systems, the perfect layer-by-layer mode is almost unexpected [10,11]. An analysis of such nonlinear AES intensity-thickness curves with existing growth models does not provide sufficiently accurate information about the initial growth stages.

Most of the existing models are based on that developed by Gallon [12]. Different approaches [2,13–15] were employed to extract the coverage of every layer, which in fact is the essential difference between the different growth modes (FM, SK, VW, SM, etc.). In the present paper, we introduce a new growth model, the diffusion-corrected simultaneous multilayer (DSCM) model, which enables quantitative interpretation of spectroscopic data as a function of thickness. The DCSM model is based on the SM model developed by Barthès *et al.* [7,16], and allows different growth modes to be distinguished. The main difference between the SM and DCSM models is the treatment of diffusion of adatoms between different layers. In this paper, we will apply the model to quantitatively interpret AES intensity-thickness data for the growth of Cr on single crystal (100) $SrTiO_3$ and (0001) α-Al_2O_3 surfaces. STM results are presented for comparison with AES data.

Depending on the material system and the growth conditions, adatoms impinging on the surface can be involved in down-step or up-step diffusion. If the impinging atoms stick only to the location on which they originally land, the adsorbate layer will develop in a statistic manner, which is described by the SM growth mode. Generally, an increase in growth temperature changes the diffusion behavior of adatoms between different layers (down-step and up-step), which affects the coverage of every individual layer. In the case of the FM mode, for example, down-step diffusion of adatoms is essential. In contrast, the VW growth mode is accompanied by up-step diffusion of adatoms (e.g., [17,18]).

In the case of the SM growth mode, the growth rate (change of coverage with time) of any particular nth layer will be proportional to the flux J of sticking adatoms and to the difference of coverage $\theta_{n-1} - \theta_n$ between the neighboring layers [7,16]:

$$\frac{d\theta_n}{dt} = J(\theta_{n-1} - \theta_n). \tag{1}$$

However, if we consider the diffusion of adatoms between different layers, the growth rate has to be modified. For any given layer, diffusion has two effects on its growth rate: Atoms, that impinge onto the specific layer and diffuse to other layers, will decrease the growth rate of this specific layer; in contrast, atoms diffusing onto a definite layer from the adjacent layers result in an increase in the growth rate of this specific layer. In reality, a single adatom has the largest probability of diffusing onto the first adjacent layer. However, to simplify the description, we have made the approximation that adatoms impinging on any layer have an identical probability of diffusing farther away to other layers. Under this assumption,

the equations for down-step and up-step diffusion are derived.

Down-step diffusion.—The decrease of the coverage of the nth layer is proportional to the amount of atoms $J(\theta_{n-1} - \theta_n)dt$ impinging on the nth layer. Furthermore, the decrease must be proportional to the uncovered area $1 - \theta_{n-1}$ below the nth layer where the atoms can diffuse away. The increase of the coverage is proportional to the amount of atoms $J\theta_n dt$ impinging onto the layers above the nth layer and to the uncovered area $\theta_{n-1} - \theta_n$ of the nth layer. For down-step diffusion, the change of coverage with time can therefore be written as $J\theta_n(\theta_{n-1} - \theta_n) - J(\theta_{n-1} - \theta_n)(1 - \theta_{n-1})$.

Up-step diffusion.—The decrease of the coverage of the nth layer is proportional to the amount of atoms impinging onto the nth layer $J(\theta_{n-1} - \theta_n)dt$ and to the uncovered region θ_n above the nth layer. The increase of the coverage of the nth layer is proportional to the number of atoms impinging onto the layers below the nth layer, $J(1 - \theta_{n-1})dt$, and to the vacant sites on the nth layer $\theta_{n-1} - \theta_n$. In analogy to the case of down-step diffusion, the change of coverage for up-step diffusion is proportional to $J(1 - \theta_{n-1})(\theta_{n-1} - \theta_n) - J(\theta_{n-1} - \theta_n)\theta_n$.

The terms for up-step and down-step diffusion have the same magnitude but opposite signs. Both terms can be combined by introducing a diffusion-corrected coefficient f, which accounts for the differences in diffusion behavior, resulting in

$$\frac{d\theta_1}{dt} = J(1 - \theta_1) + fJ(\theta_1 - \theta_1^2),$$
$$\frac{d\theta_n}{dt} = J(\theta_{n-1} - \theta_n) + fJ(\theta_{n-1}^2 - \theta_{n-1} - \theta_n^2 + \theta_n) \quad (2)$$
$$n > 1.$$

The diffusion-corrected coefficient is a measure of the fraction of adatoms diffusing up- or down-step. For down-step diffusion $0 < f < 1$ (layerlike growth), and for up-step diffusion $f < 0$ are valid (islandlike growth). For the SM growth mode, $f = 0$. $f < -1$ applies for such cases where atoms from an existing layer diffuse up-step. Equation (2) can be used to calculate the coverage of any individual layer for a given diffusion-corrected coefficient f (Fig. 1). The case of $f = 1$ [Fig. 1(a)] is similar to FM growth where the coverage of any layer increases very quickly. The rate of coverage reduces when the coverage approaches 1. This effect is similar to an increased diffusion distance for adatoms on the individual terraces. Such growth behavior is frequently observed in a variety of different systems and causes deviation from the perfect FM growth mode [7]. For $f = -1$ [Fig. 1(b)], the coverage of all layers increases very slowly, and a number of layers grow simultaneously, resulting in island growth mode. By varying only f, one can adapt the model growth behavior to the different growth modes, such as FM, SM, and VW.

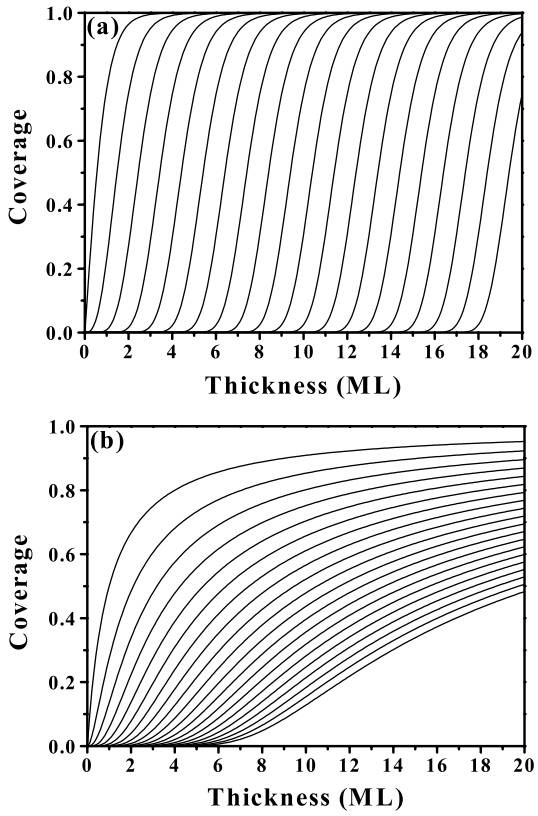

FIG. 1. Coverage $\theta_1, \theta_2, \ldots, \theta_{20}$ of the first 20 layers (first layer to 20th layer from left to right) as a function of the total dose of adatoms as calculated from different diffusion-corrected coefficients f in the DCSM model. (a) $f = 1$, layerlike mode; (b) $f = -1$, islandlike mode.

Based on the above calculation, the variations of the adsorbate and substrate Auger signals ($I_A$and I_S) can be calculated via

$$\frac{I_A}{I_A^\infty} = (1 - \alpha_A^A)[\theta_1 + \alpha_A{}^{\mathrm{A}}\theta_2 + (\alpha_A^A)^2\theta_3 + (\alpha^A{}_{\mathrm{A}})^3\theta_4 + \cdots + (\alpha_A{}^{\mathrm{A}})^n\theta_{n+1} + \cdots], \quad (3)$$

$$\frac{I_S}{I_S^0} = 1 - (1 - \alpha_S^A)[\theta_1 + \alpha_S{}^{\mathrm{A}}\theta_2 + (\alpha_S^A)^2\theta_3 + (\alpha^A{}_{\mathrm{S}})^3\theta_4 + \cdots + (\alpha_S{}^{\mathrm{A}})^n\theta_{n+1} + \cdots], \quad (4)$$

where I_A^∞ is the Auger signal from a very thick adsorbate layer, I_S^0 is the Auger signal of the clean substrate, and α_A^A and α_S^A are the transmission coefficients of Auger electrons of the adsorbate and substrate through the adsorbate matrix, respectively. In Eqs. (2)–(4), the transmission coefficient α and diffusion-corrected coefficient f are variables which allow the fitting of the experimentally determined AES signals. For example, assuming $\alpha_A^A = 0.81$, the variation of Auger signals can be calculated for different diffusion-corrected coefficients f as a function of adsorbate thickness (Fig. 2). For comparison, the curve

originating from FM growth was included in Fig. 2. Variations of f reflect the different variations of the AES signals originating from different growth modes. By fitting similar nonlinear curves with the DCSM model, quite different values of f can be obtained. A variation of f from 1 towards negative values allows one to conclude on rather layerlike, SM, and islandlike growth modes. Similar formulas [Eqs. (2)–(4)] can be used for x-ray photoelectron spectroscopy (XPS) data. LEIS data depend only on the total coverage, and can therefore be fitted by Eq. (2).

During the deposition of Cr, AES and STM measurements were carried out in a commercial multichamber molecular beam epitaxy system. Details of the system are described elsewhere [19,20]. We performed two different types of deposition experiments (i) and (ii). In experiment (i) Cr (99.99 at. %) was deposited via electron beam evaporation at room temperature and the nominal thickness was measured with a quartz balance. These films were used to calibrate the nominal film thickness via AES measurements [21]. The AES and STM measurements were performed in a chamber, which is equipped with an electrically heated evaporation source based on a tungsten filament basket [experiment (ii)]. In such experiments, the AES spectra can be recorded continuously during the evaporation of Cr via deliberate arrangement of the Cr source, the substrates, and the AES spectrometer. In this chamber, a quartz balance was again applied to monitor the growth rate. It was shown that during one deposition process (typically 30 min) no significant variation in growth rate was observed. Cr was deposited at a rate of 0.18 Å/min onto single crystal $(0001)Al_2O_3$ and $(100)SrTiO_3$ substrates under the same conditions. The substrate cleaning procedure is described elsewhere [20–22]. Considering the cube-on-cube orientation relationship of Cr on $(100)SrTiO_3$ [22] and the surface atom density of $(100)SrTiO_3$ (1.31×10^{15} cm^{-2}), one monolayer of Cr corresponds to a thickness of 1.58 Å. AES spectra were recorded with a double-pass cylindrical mirror analyzer at a constant flux of 20 μA of primary electrons and a primary energy of 3 keV. Auger signals from the substrate and Cr overlayer were recorded in the direct $EN(E)$ mode and the spectra were differentiated to obtain the Auger peak-to-peak heights (APPH). The common Auger transitions of Cr LVV (571 eV) and O KLL (503 eV) were taken as the signals from the adsorbate and substrates, respectively. LVV and KLL denote Auger processes involving the K, L, and V shells. All STM measurements were conducted with Pt-Ir tips at a tunneling voltage $U_t = 1 \sim 2$ V and tunneling currents $I_t = \sim 0.2$–0.5 nA.

Figure 3 shows the Auger signals as a function of Cr thickness. The APPH values of Cr and O have been normalized by the intensity values recorded from thick

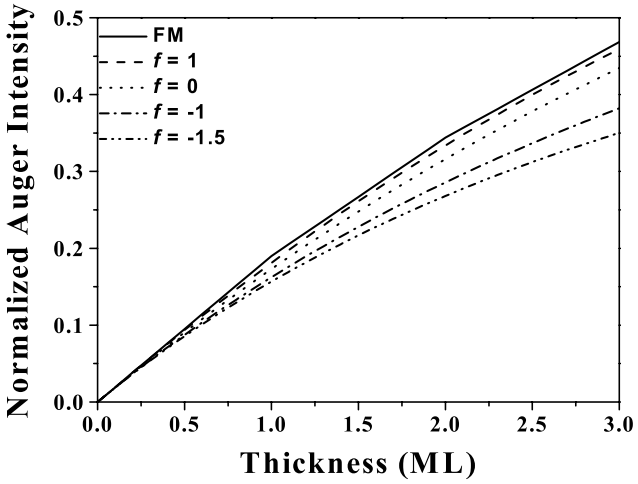

FIG. 2. The calculated variation of Auger signals with thickness, using different diffusion-corrected coefficients f. The transmission coefficient α was taken as 0.81.

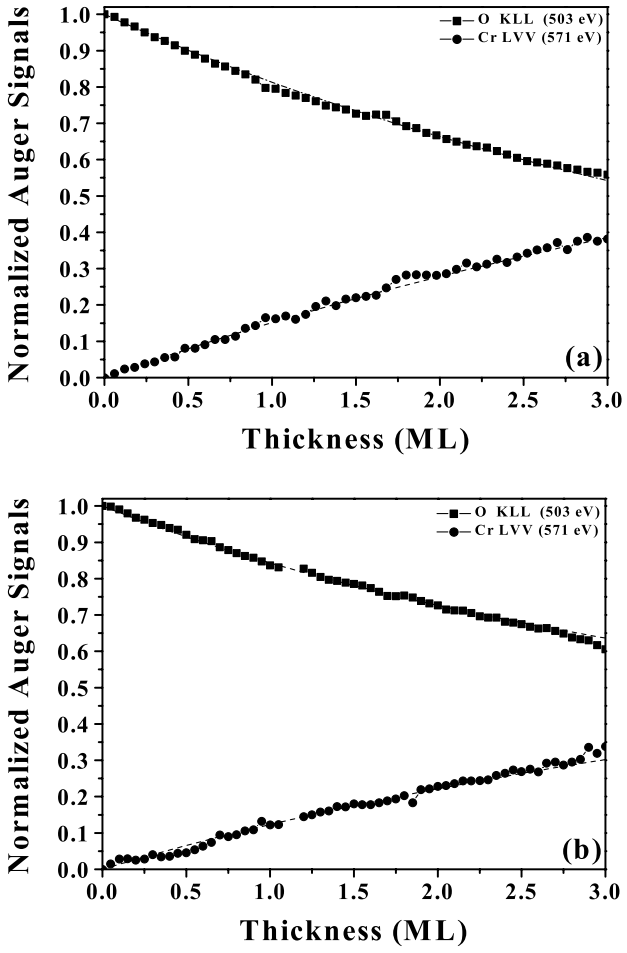

FIG. 3. Normalized Auger peak-to-peak height for Cr LVV (571 eV) and O KLL (503 eV) spectra plotted as a function of Cr coverage. (a) Cr deposition on (100) $SrTiO_3$ at room temperature; (b) Cr deposition on (0001) Al_2O_3 at room temperature. The dashed lines are the curves fitted using the DCSM model (see text).

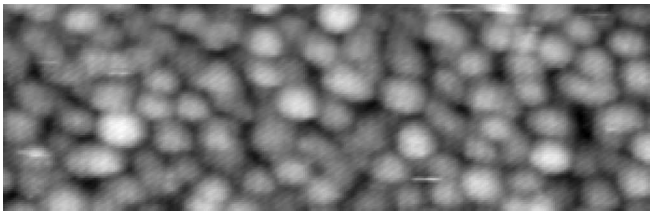

FIG. 4. 19 nm × 60 nm STM image of a Cr layer (clusters) deposited on (100) $SrTiO_3$ at room temperature (0.4 nm nominal thickness).

Cr films ($I^{\infty}_{Cr,Cr/SrTiO_3}$ and $I^{\infty}_{Cr,Cr/Al_2O_3}$), and the corresponding clean $SrTiO_3$ ($I^{\infty}_{O,SrTiO_3}$) and Al_2O_3 (I^{∞}_{O,Al_2O_3}) substrates, respectively.

The absence of breaks in the curves alone does not exclude the operation of the FM growth mode. In the $Cr/SrTiO_3$ and Cr/Al_2O_3 systems, AES signals at the same rate scale present different variations with thickness in Figs. 3(a) and 3(b). Fitting both curves with the SM model resulted in fully different transition coefficients α^{Cr}_{Cr} and α^{Cr}_{O}, which, however, should be identical. By fitting the data with the DCSM model, i.e., Eqs. (2)–(4), the variables f and α can be determined. The inelastic mean-free paths λ of AES electrons can be calculated using the formula from Seah *et al.* [23] or the TPP-2 formula [24] resulting in $\lambda = (13 \pm 1)$ Å and $\lambda = (11 \pm 1)$ Å for the Cr LVV (571 eV) and O KLL (503 eV) Auger electrons passing through a Cr matrix. Following the definition of λ, the transition coefficient α can be calculated from the expression $\lambda = d_m/(1 - \alpha)\cos\beta$ [9] ($d_m = 1.58$ Å; $\beta = 42°$ is the effective mean acceptance angle of the analyzer) as $\alpha^{Cr}_{Cr} = 0.835 \pm 0.015$ and $\alpha^{Cr}_{O} = 0.805 \pm 0.02$. Our best fit with the DCSM model (dashed lines in Fig. 3) resulted in $f_{Cr/SrTiO_3} = -0.2 \pm 0.1$, $\alpha^{Cr}_{Cr} = 0.835$, and $\alpha^{Cr}_{O} = 0.79$ for the $Cr/SrTiO_3$ system, and $f_{Cr/Al_2O_3} = -1.2 \pm 0.1$, $\alpha^{Cr}_{Cr} = 0.86$, and $\alpha^{Cr}_{O} = 0.815$ for the Cr/Al_2O_3 system, respectively. The transmission coefficients obtained from the DCSM simulation and those calculated above are in good agreement for both systems. $f < 0$ indicates that Cr grows in the form of islands on both substrates. For identical coverage, a more negative value of f corresponds to a lower density of Cr islands and/or less complete wetting. For example, equal island densities in the $Cr/SrTiO_3$ and Cr/Al_2O_3 systems would lead to the conclusion that Cr is wetting the $SrTiO_3$ surface better than the Al_2O_3 surface, which corresponds to a higher interfacial energy for the Cr/Al_2O_3 system or to weaker interfacial bonding.

Figure 4 shows a STM image of Cr clusters on the (100) surface of $SrTiO_3$ after deposition of a nominal thickness of 0.4 nm of Cr. As expected from AES measurements, Cr exhibits VW growth.

In summary, we have shown that the DCSM model is a useful tool to obtain quantitative information about the initial stage of thin film growth, especially in the case of island growth. The magnitude of the diffusion-corrected coefficient f is a direct measure of the interaction between overlayers and substrates. The model can be applied to fit experimental results based on AES, XPS, and LEIS measurements or other *in situ* spectroscopic observations of thin film growth.

The authors thank S. Hofmann for stimulating discussions. M. Pudleiner is acknowledged for help with the MBE experiments.

*Corresponding author.
Email address: wagner@mf.mpg.de

[1] K. H. Ernst, A. Ludviksson, R. Zhang, J. Yoshihara, and C. T. Campbell, Phys. Rev. B **47**, 13 782 (1993).
[2] U. Diebold, J. M. Pan, and T. E. Madey, Phys. Rev. B **47**, 3868 (1993).
[3] L. Zhang, R. Persaud, and T. E. Madey, Phys. Rev. B **56**, 10 549 (1997).
[4] C. Xu, X. Lai, G.W. Zajac, and D.W. Goodman, Phys. Rev. B **56**, 13 464 (1997).
[5] M. C. Gallagher, M. S. Fyfield, and S. A. Joyce, Phys. Rev. B **59**, 2346 (1999).
[6] D. A. Chen, M. C. Bartelt, R. Q. Hwang, and K. F. McCarty, Surf. Sci. **450**, 78 (2000).
[7] C. Argile and G. E. Rheed, Surf. Sci. Rep. **10**, 277 (1989).
[8] S. Mróz and A. Mróz, Thin Solid Films **367**, 126 (2000).
[9] G. E. Rhead, M. G. Barthès, and C. Argile, Thin Solid Films **82**, 201 (1981).
[10] J. H. Larsen, J. T. Ranney, D. E. Starr, J. E. Musgrove, and C. T. Campbell, Phys. Rev. B **63**, 195410 (2001).
[11] C. Goyhenex, M. Meunier, and C. R. Henry, Surf. Sci. **350**, 103 (1996).
[12] T. E. Gallon, Surf. Sci. **17**, 486 (1969).
[13] R. Memeo, F. Ciccacci, C. Mariani, and S. Ossicini, Thin Solid Films **109**, 159 (1983).
[14] F. C. M. J. M. van Delft, A. D. van Langeveld, and B. E. Nieuwenhuys, Thin Solid Films **123**, 333 (1985).
[15] M. Volpe, M. Tomelloni, and M. Fanfoni, Surf. Sci. **423**, L128 (1999).
[16] M. G. Barthès and A. Rolland, Thin Solid Films **76**, 45 (1981).
[17] T. R. Linderoth, S. Horch, L. Pertersen, S. Helveg, E. Lægsgaard, I. Stensgaard, and F. Besenbarcher, Phys. Rev. Lett. **82**, 1494 (1999).
[18] F. Montalenti and R. Ferrando, Phys. Rev. Lett. **82**, 1498 (1999).
[19] J. Marien, T. Wagner, G. Duscher, A. Koch, and M. Rühle, Surf. Sci. **446**, 219 (2000).
[20] Q. Fu and T. Wagner, Surf. Sci. **505**, 39 (2002).
[21] S. Bernath, T. Wagner, S. Hofmann, and M. Rühle, Surf. Sci. **400**, 335 (1998).
[22] Q. Fu and T. Wagner, Thin Solid Films **420–421**, 455 (2002).
[23] M. P. Seah and W. A. Dench, Surf. Interface Anal. **1**, 2 (1979).
[24] S. Tanuma, C. J. Powell, and D. R. Penn, Surf. Interface Anal. **17**, 911 (1991).